

Research Article

Sorbents Coupled to Solar Light TiO_2 -Based Photocatalysts for Olive Mill Wastewater Treatment

Andrea Speltini,¹ Federica Maraschi,¹ Michela Sturini,¹ Valentina Caratto,²
Maurizio Ferretti,² and Antonella Profumo¹

¹Department of Chemistry, University of Pavia, Via Taramelli 12, 27100 Pavia, Italy

²Department of Chemistry and Industrial Chemistry, University of Genoa, Via Dodecaneso 31, 16146 Genova, Italy

Correspondence should be addressed to Antonella Profumo; antonella.profumo@unipv.it

Received 24 February 2016; Accepted 30 June 2016

Academic Editor: Juan M. Coronado

Copyright © 2016 Andrea Speltini et al. This is an open access article distributed under the Creative Commons Attribution License, which permits unrestricted use, distribution, and reproduction in any medium, provided the original work is properly cited.

The aim of this work was to couple physical-chemical approaches with photocatalysis to reduce by a simple, inexpensive way the organic load of olive mill wastewater (OMW), mandatorily prior to the final discharge. Before irradiation, different sorbents were tested to remove part of the organic fraction, monitored by measuring chemical oxygen demand (COD) and polyphenols (PP). Different low-cost, safe materials were tested, that is, Y zeolite (ZY), montmorillonite, and sepiolite. Considerable decrease of organic load was obtained, with the highest abatement (40%) provided by ZY (10 g L⁻¹ in 1:10 OMW). Use of the three sorbents, in particular ZY, was convenient compared to commercial activated carbons. UV light photocatalytic tests, performed using P25 TiO₂ on ZY-treated OMW, yielded quantitative remediation (ca. 90%). Also solar light provided significant results, PP being lowered by 74% and COD by 56%. Sol-gel anatase TiO₂ and N-doped anatase TiO₂ were also tested, obtaining good results, around -80% PP and -40% COD. Finally, an integrated approach was experimented by ZY-supported anatase TiO₂ (TiO₂@ZY). This *photoreactive sorbent* allowed *one-pot* treatment of OMW significant abatements of PP (-77%) and COD (-39%) with only 1 g L⁻¹ material, under solar light.

1. Introduction

Olive mill wastewater (OMW) is a highly toxic effluent obtained from the extraction process of the olive oil industry and is considered an undesired waste. OMW represents a serious problem in the Mediterranean basin [1], as over 95% of the world production, estimated at more than 30 million m³ [2], occurs in Mediterranean countries and about 80% in the European Union, mainly Spain, Italy, and Greece [3]. It has been calculated that the volume of OMW coming from milling activity ranges from 0.5 to 1.5 m³ per ton of olives [3].

The OMW is a blackish liquid containing 80–83% of water (pH around 4.5), organic compounds ranging from 40 to 220 g L⁻¹ [2]. As expectable, the composition is variable and depends on many factors, namely, olive cultivar, extraction process, and climatic conditions, but always includes oil and grease, sugars, polyalcohols, pectins, lipids, and polyphenols

(PP) [4, 5]. Specifically, it has been reported that more than 30 phenolic compounds are present in OMW [6]. Beside lignin and tannins, the high content of phenolic species in a wide range of molecular weights is responsible for the typical black-brownish colour [4]. The dark colour of the OMW disturbs the sunlight absorption by photosynthetical organisms whereas the surface oil film prevents the oxygen absorption from air releasing an intense smell.

OMW is indeed considered a source of environmental pollution, due to the high levels of PP, persistent phytotoxic and antibacterial compounds that inhibit biodegradation. Due to the high content of phenols and long-chain fatty acids, high values of chemical oxygen demand (COD), up to 200 g L⁻¹, and biochemical oxygen demand (up to 100 g L⁻¹) are expected [3, 5]. Since these values may be found as hundreds of times higher than those of typical municipal sewage [7], it is clear that a direct discharge in receiving waters or soils is not possible because it would involve severe

effects, that is, ecotoxicity and eutrophication for natural water bodies.

Although the complex organic composition of OMW has been recently exploited to obtain “clean energy,” such as hydrogen gas [1, 3, 8], the actual major issue is the development of efficient, simple, and low environmental impact treatments for OMW before the final discharge.

Among the methods used for OMW treatment, physico-chemical treatments (i.e., settling, centrifugation, and filtration) coupled with adsorption on activated carbon have been practiced [9]. On the other side, the biological treatments, mainly consisting of anaerobic digestion [10], require large dilution factors or mandatory dephenolization procedures [11]. Advanced oxidation processes (AOPs) by ozonization [12] or photo-Fenton [5, 13–16] have been experimented, and integrated approaches involving flocculation/coagulation and/or adsorption, enzymatic, and biological treatments and photocatalysis have been proposed [5, 13–15, 17]. However, an environmentally safe and cost-effective solution to OMW treatment is still lacking [18].

Heterogeneous photocatalysis, requiring just a semiconductor and a light source, is a very promising, environmentally benign way to reduce the toxic organic load of OMW, as reported in some recent studies [14, 15, 17, 19, 20]. As for photo-Fenton applied to OMW [5], it seems convenient to design a sequential procedure combining pretreatment of the raw OMW, by adsorption onto high surface area sorbents, with a photocatalytic treatment and/or a biological step before the final discharge. As a matter of fact, photocatalysis is becoming increasingly attractive for environmental remediation [21], for instance, for abatement of emerging organic pollutants [22] or toxic metals [23], but also for OMW remediation [14, 15, 17, 19]. Owing to chemical stability, efficiency, low cost, and nontoxicity, titanium dioxide (TiO_2) is the most used photocatalyst, recently applied also for OMW remediation, after immobilization onto sepiolite [19]. However, to the authors' best knowledge, the application of N-doped TiO_2 or ZY-supported TiO_2 has not been reported in the literature for OMW treatment.

Based on this background, the aim of this work was to find out a simple and efficient procedure for the abatement of the organic load of OMW, in particular COD and PP levels. These were the two key parameters for evaluating the efficiency of the various treatments tested, that is, flocculation/coagulation, adsorption, and photocatalysis. Different high surface area materials were employed in the adsorption step, namely, Y zeolite (ZY), sepiolite (SEP), and montmorillonite (MMT), in addition to two commercially available activated carbons. After adsorption, OMW was submitted to photocatalytic treatment, under both UV and solar light. Different semiconductors were investigated, namely, anatase TiO_2 and N-doped anatase TiO_2 prepared by sol-gel method and characterized before use and commercial P25 TiO_2 . Finally, a hybrid material consisting of ZY-supported anatase TiO_2 combining sorption capacity and photocatalytic activity was prepared, characterized, and tested as *photoreactive sorbent* for the *one-pot* treatment of OMW, under solar light.

2. Experimental Procedure

2.1. Chemicals. $\text{AlCl}_3 \cdot 6\text{H}_2\text{O}$ (99%), $\text{Ca}(\text{OH})_2$ ($\geq 95\%$), cetylpyridinium bromide (CPB, 98%), Folin-Ciocalteu's phenol reagent (2N), gallic acid (98%) and Y zeolite (ZY), titanium (IV) tetraisopropoxide (97% v/v), and 2-propanol (99.5% v/v) were obtained from Sigma-Aldrich (Milan, Italy). $\text{Na}_2\text{CO}_3 \cdot 10\text{H}_2\text{O}$ (99.5%) was purchased from Carlo Erba Reagents (Milan, Italy) and Superfloc C 1598, a cationic emulsion polyacrylamide, from Kemira. AC20G (0.6–2.4 mm) and F-300 (0.8–1 mm) activated carbons were acquired from Puro-lite (Llantrisant, UK) and Chemviron Carbon Ltd. (Ashton-in-Makerfield, UK), respectively. SP-1 sepiolite (SEP, 50 grm/unit), Valdemoro, Spain (Miocene age, containing minor calcite), and Camontmorillonite STx-1 (MMT) were obtained from Clay Mineral Society; physical-chemical properties can be found at <http://www.clays.org/Sourceclays.html>. Evonik P25 TiO_2 (80% anatase, 20% rutile, particle size 30 nm, and surface area $50 \pm 15 \text{ m}^2 \text{ g}^{-1}$) was purchased from Evonik Industries AG (Hanau, Germany). Distilled water was produced in laboratory.

2.2. Olive Mill Wastewater. OMW was collected at the outlet of an olive mill located in Recco, near Genova (Italy). Samples were taken using PET containers and stored in the dark (-20°C). Before use, aliquots of each sample were mixed to obtain a homogeneous representative sample, submitted to centrifugation ($3 \times 10 \text{ min}$ at 4500 rpm, Sigma 2-16P Celbio Spa centrifuge) to remove suspended solids and oil residues [5]. The resulting matrix was then characterized having pH 5.1, conductivity at 20°C 8.21 mS cm^{-1} , COD $52500 (1530) \text{ mg L}^{-1} \text{ O}_2$, and total PP content $3444 (114) \text{ mg L}^{-1}$. These values, the mean of three replicates, are typical of OMW [5, 8, 14, 24]. The OMW sample was stored in the dark (4°C) and successively used to test the various chemical-physical and photocatalytic treatments.

2.3. Analytical Determinations. COD was determined before and after treatment according to the ISO 15705 protocol. The commercialized Hach Lange kit was used, working in the concentration interval $0\text{--}1000 \text{ mg L}^{-1} \text{ O}_2$. After incubation of the sample (2 h, 148°C , LT200 thermostat), COD quantification was performed by the standardized Hach Lange spectrophotometer (DR3900).

Total PP were determined according to the Folin-Ciocalteu method. A proper sample aliquot was placed in a 10 mL volumetric flask, and 0.5 mL of the Folin-Ciocalteu reagent was added, followed by 1 mL of Na_2CO_3 (20%, w/v), and made up to 10 mL with distilled water. The control sample (no OMW) was prepared separately. The flasks were allowed to stand for 1 h; then, spectrophotometric measurements were performed at 700 nm (UVmini-1240 Shimadzu Corporation). Quantification was carried out by external calibration analyzing gallic acid standard solutions in the concentration range $2\text{--}8 \text{ mg L}^{-1}$ (linearity $r^2 > 0.9975$, three independent calibration curves).

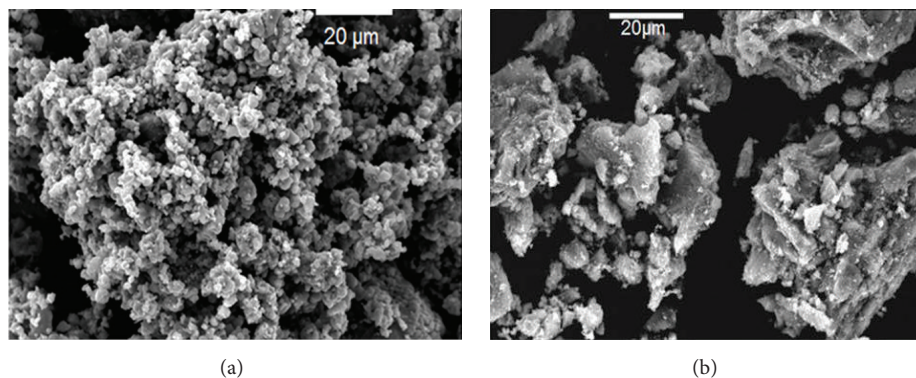


FIGURE 1: SEM images collected on anatase TiO_2 (a) and N-doped anatase TiO_2 (b).

2.4. Pretreatment by Chemical Reagents. To test the potential effect of coagulant/flocculant agents, 30 mL of centrifuged OMW was spiked with $30\ \mu\text{L}$ of 1% w/v AlCl_3 solution and then the sample was basified (pH 8) by addition of 5% w/v $\text{Ca}(\text{OH})_2$ solution. Alternatively, the OMW sample was enriched with $0.5\ \text{g L}^{-1}$ cationic organic polyelectrolyte. In both cases, the sample was maintained under magnetic stirring overnight and then centrifuged (20 min, 4500 rpm) and filtered (nylon membrane, $0.45\ \mu\text{m}$) before COD and PP determination.

2.5. In-Batch Sorption Pretreatment. In the case of commercial granular activated carbons, batch sorption experiments were conducted on 30 mL OMW in the presence of $10/100\ \text{g L}^{-1}$ of each sorbent. The suspensions were shaken on a rotating plate (150 rpm) in polypropylene tubes, at room temperature for 24 h. The same procedure was followed in the case of ZY ($10\text{--}40\ \text{g L}^{-1}$), SEP, and MMT ($10\ \text{g L}^{-1}$), using OMW (1:10). SEP was also tested after derivatization with CPB [25]. After equilibration, the suspensions were centrifuged (10 min, 4500 rpm) and then filtered by a nylon membrane ($0.45\ \mu\text{m}$) before COD and PP determination.

2.6. Photocatalysts: Synthesis and Characterization. Beside the commercial P25 TiO_2 , other TiO_2 -based photocatalysts were tested. TiO_2 and N-doped TiO_2 have been synthesized by sol-gel process. According to previous work [26], titanium isopropoxide, isopropanol, and water have been used as precursors with the same concentrations reported changing the different solution to H_2O for TiO_2 and $\text{H}_2\text{O-NH}_3$ for TiO_2 doped nanoparticles.

$\text{TiO}_2@\text{ZY}$ has been synthesized according to Maraschi et al. [27]. The sample was obtained by magnetically stirring the resultant suspension of amorphous TiO_2 mixed with H^+ zeolite (2:1 w/w) in water. Powder was filtered, washed, and finally dried. Nominally, 1.5 g of the hybrid sample contains 1 g of nanometric TiO_2 .

The synthesized samples have been finally treated in a muffle furnace (Carbolite RHF1400) at 350°C for 1 hour to promote amorphous to anatase phase conversion.

The samples have been analyzed by X-ray powder diffraction (XRPD), scanning electron microscopy (SEM), diffuse

reflectance spectroscopy (DRS), and Brunauer-Emmett-Teller analysis (BET). Phase identification was performed by XRPD analysis using a Philips PW1830 diffractometer (Bragg-Brentano geometry; $\text{Cu K}\alpha$; Ni filtered; range $20\text{--}80\ 2\theta$; step $0.025\ 2\theta$; sampling time 10 s). SEM was performed using a Tescan Vega 3 XMV microscope on powders coated with gold in low vacuum. DRS was performed using a Perkin Elmer UV-Vis spectrophotometer LAMBDA 35 equipped with an integrating sphere. BET analysis was carried out using an ASAP 2010 physisorption analyzer (Micromeritics Instrument Corp). Before measurements, the samples were pretreated at 200°C in vacuum. Ar was used for ZY, while N_2 was used for all other materials.

2.7. Photocatalytic Irradiation. All the photocatalytic experiments were performed on 10 mL ZY-treated OMW (see Section 2.5) in the presence of $1\ \text{g L}^{-1}$ of P25 TiO_2 , anatase TiO_2 , and anatase N- TiO_2 . For ZY-supported TiO_2 , any previous adsorption was done. Suspensions were irradiated (8 h) under UV light or simulated solar light. For UV irradiation, samples were placed in quartz tubes and treated under continuous air insufflation at 254 nm ($4 \times 15\ \text{W}$ lamps) or 310 nm ($10 \times 15\ \text{W}$ lamps). In the case of solar light, samples were placed in Pyrex glass containers and irradiated under magnetic stirring. A solar Box 1500e (CO.FO.ME.GRA S.r.l., Milan, Italy) set at a power factor of $500\ \text{W m}^{-2}$ and equipped with a UV outdoor filter of soda lime glass IR treated was used as the solar light simulator. After photocatalysis, each sample was filtered and COD and PP concentrations were checked.

3. Results and Discussion

3.1. Characterization of the Prepared Photocatalysts. XRD spectra of TiO_2 , N-doped TiO_2 , and $\text{TiO}_2@\text{ZY}$ confirm the presence of anatase crystalline structure (Figure S1 in Supplementary Material available online at <http://dx.doi.org/10.1155/2016/8793841>). The SEM analysis shows the morphology of the samples. Undoped TiO_2 grains have rounded shape and form sponge-like aggregates (Figure 1(a)), while the N-doped ones form lamellar isolated aggregates (Figure 1(b)), in accordance with literature [26].

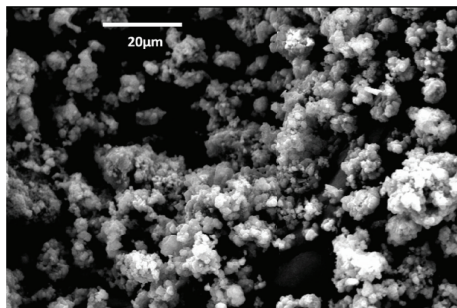


FIGURE 2: SEM image collected on the photoreactive sorbent anatase $\text{TiO}_2@ZY$.

TABLE 1: Values of absorption wavelength, energy gap, and BET surface area determined for each material.

Sample	Absorption wavelength (nm)	Energy gap (eV)	Surface area ($\text{m}^2 \text{g}^{-1}$)
Anatase TiO_2	384	3.2	120
N-doped anatase TiO_2	413	3.0	67
$\text{TiO}_2@ZY$	384	3.2	216
ZY	188	3.7	175

The TiO_2 nanoparticles supported by the zeolite are round shaped (Figure 2) and the sample is homogenous, as previously reported by Maraschi et al. [27]. The values of absorption wavelength, energy gap, and surface area of each material are reported in Table 1. It is apparent that N-doping yields a narrower band gap compared to anatase TiO_2 , although the latter shows a twofold higher surface area. The DRS spectra of doped and undoped TiO_2 are shown in the supplementary information (Figure S2). The E_{gap} calculation was made according to literature [26, 28]. The composite material, $\text{TiO}_2@ZY$, shows the highest surface area ($>200 \text{ m}^2 \text{ g}^{-1}$); the smaller energy gap and higher surface area compared to pristine ZY confirm the successful immobilization of the photocatalyst onto the zeolitic structure.

BET analyses are in agreement with the literature data [27].

3.2. OMW Treatment: Adsorption Coupled to Photocatalysis.

A first series of experiments was carried out to further reduce the suspended particles of the centrifuged OMW prior to the photocatalytic step, which is more efficient in limpid solution due to higher light penetration and lower scattering phenomena [14]. Since use of chitosan (0.4 g L^{-1}) before Fenton and photo-Fenton oxidation was reported [15], some experiments were performed in the presence of less expensive agents, either AlCl_3 (0.001%, v/v) under alkaline conditions (pH 8) or cationic organic polyelectrolyte (0.5 g L^{-1}), in order to test the potential effects of coagulation/flocculation in removing colloids ($<1 \mu\text{m}$). Results showed that both treatments yielded a COD abatement lower than 10%, whereas a 36% decrease of PP was observed using AlCl_3 , indicating that the sole

centrifugation is convenient for removing suspended organic matter.

To reduce the organic load of OMW, in-batch sorption was therefore exploited as a possible more efficient approach, investigated in the recent years for OMW treatment [5, 24, 29]. ZY, MMT, and SEP, largely available and low-cost materials characterized by high surface area, were selected as in principle they can operate in very complex matrices like OMW [5, 24, 29].

ZY (surface area $175 \text{ m}^2 \text{ g}^{-1}$) was tested in the concentration range $10\text{--}40 \text{ g L}^{-1}$, working at the sample native pH, and results are shown in Table 2.

COD and PP levels were substantially lowered after contact with ZY, indicating a strong affinity for the organic constituents of OMW. This is in accordance with literature data reporting on the use of zeolites for wastewater treatment [4, 29]. No significant improvement was seen in going from the lowest to the highest ZY concentration; thus, 10 g L^{-1} seemed convenient.

Despite the good results obtained, 1:10 diluted OMW was used for further experiments (see Table 3), in order to dispose of a final solution suitable for the photocatalytic treatment [15, 20]. Indeed, photocatalysis cannot operate satisfactorily in not diluted OMW, as later described and in agreement with literature [14]. The efficiency of ZY was then compared to clay powders, namely, SEP (surface area $213 \text{ m}^2 \text{ g}^{-1}$) and MMT (surface area $84 \text{ m}^2 \text{ g}^{-1}$), under the above reported conditions. These were tested because clays proved to be effective for purification of urban and industrial wastewater and have been recently employed also in the case of OMW [5, 29, 30].

As reported in Table 3, PP level dropped down by ca. 40% after adsorption onto SEP and MMT, similar to the case of ZY, and COD by ca. 30%.

With the aim of further improving ZY efficiency, the crude powder was derivatized with CPB, a cationic surfactant that could favour sorption of polyphenolic species [25]. However, no significant improvement in PP removal was observed using the CPB-derivatized material; thus, it was preferred to use the raw ZY.

Since activated carbon is the most used sorbent for water and wastewater purification, two types of granular activated carbon, specifically AC20G and F-300, were tested for comparison. Due to the large surface area ($>1000 \text{ m}^2 \text{ g}^{-1}$) and strong binding affinity of these materials for organic compounds, experiments were performed on not diluted OMW, using 100 g L^{-1} sorbent, and on 1:10 OMW with 10 g L^{-1} sorbent obtaining comparable results (see Tables 2 and 3).

Nevertheless, considering the results obtained by using the alternative sorbents (10 g L^{-1} , 1:10 OMW, Table 3) and their low cost compared to activated carbon, ZY proved to be a valid sorbent for OMW remediation and was therefore selected as the convenient adsorbent phase to treat OMW prior to the photocatalytic irradiation. Indeed, after ZY-contact, a biological step followed by an AOP treatment would be required to reach remediation of OMW, or as in this case, the treated OMW can be directly submitted to

TABLE 2: PP and COD values in OMW before and after adsorption onto ZY and activated carbons ($n = 3$).

Sample	PP (mg L ⁻¹)	Abatement (%)	COD (mg L ⁻¹ O ₂)	Abatement (%)
OMW	3444 (114)	—	52500 (1530)	—
OMW + ZY (10 g L ⁻¹)	2431 (170)	30 (5)	35900 (1424)	32 (3)
OMW + ZY (20 g L ⁻¹)	2189 (152)	37 (4)	32846 (1462)	37 (4)
OMW + ZY (40 g L ⁻¹)	1877 (150)	46 (4)	29300 (1568)	44 (3)
OMW + AC20G (100 g L ⁻¹)	617 (76)	82 (2)	18800 (1945)	64 (4)
OMW + F-300 (100 g L ⁻¹)	1130 (114)	67 (3)	22200 (2054)	58 (4)

TABLE 3: PP and COD values in 1:10 OMW before and after adsorption onto 10 g L⁻¹ ZY, CPB/ZY, SEP, MMT, and activated carbons ($n = 3$).

Sample	PP (mg L ⁻¹)	Abatement (%)	COD (mg L ⁻¹ O ₂)	Abatement (%)
1:10 OMW	335 (25)	—	5226 (330)	—
1:10 OMW + ZY (10 g L ⁻¹)	186 (21)	44 (6)	2640 (258)	36 (3)
1:10 OMW + CPB/ZY (10 g L ⁻¹)	194 (19)	42 (5)	2637 (247)	49 (4)
1:10 OMW + SEP (10 g L ⁻¹)	210 (17)	37 (5)	3685 (147)	29 (3)
1:10 OMW + MMT (10 g L ⁻¹)	209 (13)	38 (4)	3220 (161)	38 (3)
1:10 OMW + F-300 (10 g L ⁻¹)	111 (9)	77 (6)	2561 (237)	51 (5)
1:10 OMW + AC20G (10 g L ⁻¹)	121 (11)	74 (6)	2770 (232)	47 (4)

TABLE 4: PP and COD values in 1:10 OMW before and after photocatalytic treatment under UV and solar simulated light using P25 TiO₂ ($n = 3$).

Sample	PP (mg L ⁻¹)	Abatement (%)	COD (mg L ⁻¹ O ₂)	Abatement (%)
1:10 OMW	335 (25)	—	5226 (330)	—
1:10 OMW + ZY (10 g L ⁻¹)	186 (21)	44 (6)	2640 (258)	36 (3)
1:10 OMW + ZY (10 g L ⁻¹) + P25 TiO ₂ (254 nm) ^a	21 (3)	94 (1)	490 (39)	91 (1)
1:10 OMW + ZY (10 g L ⁻¹) + P25 TiO ₂ (310 nm) ^a	31 (4)	91 (1)	775 (54)	85 (1)
1:10 OMW + ZY (10 g L ⁻¹) + P25 TiO ₂ (solar box) ^a	87 (7)	74 (5)	1585 (127)	56 (2)

^a1 g L⁻¹ photocatalyst, 8 h irradiation.

photocatalysis. This was investigated under either UV or solar simulated light, using commercial P25 TiO₂ and sol-gel anatase TiO₂ and N-doped anatase TiO₂, the two latter not being previously investigated for OMW.

Irradiation in presence of the former semiconductor led to quantitative abatements, around 90%, working under UV light. Interesting data were found also under solar simulated irradiation, with COD and PP decrease of 56% and 74%, correspondingly (see Table 4).

Notice that the adsorption step prior to photocatalysis is of great importance in allowing a successful remediation of OMW. Indeed, direct photocatalytic treatment on 1:10 OMW (not contacted with ZY) led to a COD abatement of just 20% even under drastic conditions (254 nm, 8 h radiation). On the other hand, irradiation of not diluted OMW after ZY-adsorption was as well unsuccessful. As shown in UV-Vis spectra of OMW samples (see Figure S3, Supplementary Materials), the sorption step on ZY is convenient not only for PP/COD abatement, but also to favour light penetration by decreasing the sample absorbance (ca. 20%).

These findings support the actual reports on TiO₂ photocatalytic treatment of OMW, requiring a diluted sample [14, 15, 17]. Nevertheless, dilution can be avoided in the case of photo-Fenton, but the additional costs due to the use of

oxidizing reagents and necessity to adjust pH have to be taken into account [13, 14, 16]. Besides, since photo-Fenton was shown to preserve or even increase the OMW effluent toxicity, a successive biotreatment that would be required to further reduce COD and phenols could be hampered [16].

The adsorption-photocatalysis combined treatment on 1:10 OMW presented here is convenient and efficient, as the PP content was reduced to ca. 20 mg L⁻¹, and COD was lowered below the limit (500 mg L⁻¹) indicated by the actual Italian legislation for wastewater discharge. The above results were substantiated by control experiments performed to evaluate the role of direct photolysis that is in the absence of catalyst, under the same conditions. COD and PP reduction being lower than 10%, except in the case of 254 nm for PP (-29%), these findings absolutely attest the great contribution of the photocatalyst in degrading OMW organics.

In the framework of the photochemical step, a part of the work was undertaken to strengthen the possibility of working under solar light and, with this aim, N-doped anatase TiO₂ was tested, compared to anatase TiO₂ as the control sample. Indeed, the absorption edge of P25 TiO₂ is around 390 nm, in relation to its band gap of 3–3.2 eV; thus, just the 5% of the solar light spectrum can be exploited for the activation of the semiconductor. Differently, a red-shift absorption of TiO₂

TABLE 5: PP and COD values in 1:10 OMW before and after photocatalytic treatment under solar simulated light using different TiO₂-based photocatalysts ($n = 3$).

Sample	PP (mg L ⁻¹)	Abatement (%)	COD (mg L ⁻¹ O ₂)	Abatement (%)
1:10 OMW	335 (25)	—	5226 (330)	—
1:10 OMW + ZY (10 g L ⁻¹)	186 (21)	44 (6)	2640 (258)	36 (3)
1:10 OMW + ZY (10 g L ⁻¹) + P25 TiO ₂ ^a	87 (7)	74 (5)	1585 (127)	56 (2)
1:10 OMW + ZY (10 g L ⁻¹) + anatase TiO ₂ ^a	54 (5)	84 (6)	3031	42 (3)
1:10 OMW + ZY (10 g L ⁻¹) + N-doped anatase TiO ₂ ^a	74 (6)	78 (4)	3188	39 (3)
1:10 OMW + TiO ₂ @ZY ^a	77 (6)	77 (3)	3170 (224)	39 (3)

^a1 g L⁻¹ photocatalyst, 8 h irradiation.

can be achieved after derivatization or doping [31]. Despite the narrower band gap obtained after N-doping (3.0 eV), the efficiency in degrading OMW organics was comparable to anatase TiO₂ (band gap 3.2 eV), as shown in Table 5.

This is reasonably attributable to the lower surface area of the N-doped particles that could be improved with further optimization of the synthesis. Anyway, as apparent from Table 5, both sol-gel semiconductors are attractive under solar light compared to commercial P25 TiO₂.

Further experiments were planned using a hybrid material able to join sorption capability and photocatalytic activity, that is, TiO₂@ZY. As shown in Table 5, TiO₂@ZY proved to be greatly advantageous because it allowed the same efficiency in terms of PP/COD abatement, compared to the sequential treatment entailing adsorption on ZY and photocatalytic steps. Use of this sorbent/photoreactive material provides those similar satisfying results by one-pot treatment and tenfold lower amount of material.

The overall abatement is indeed due to the sorption capacity of this composite (49% PP and 29% COD) combined with the photocatalytic properties (further abatement 28% PP and 10% COD). This behavior can be certainly explained by considering the physical-chemical properties of the composite. Indeed, among the many factors that may influence the photocatalytic activity, namely, crystal structure, energy gap, and surface area, TiO₂@ZY presents as well greater surface area with respect to pristine zeolite, anatase TiO₂, and N-doped TiO₂, due to the smaller regular dimension of grains combined with the high surface area of ZY.

4. Conclusions

A simple, working procedure for OMW treatment prior to final discharge, entailing adsorption onto Y zeolite followed by TiO₂ photocatalysis, is described here. The first step allowed relevant abatement of the organic load of OMW due to adsorption onto ZY, a largely available and costless material, providing an intermediated sample suitable to be submitted to photocatalytic treatment. This was studied under both UV and simulated solar light, in presence of various TiO₂-based photocatalysts, namely, commercial P25, sol-gel anatase, and sol-gel N-doped anatase TiO₂. Photocatalysis proved to degrade substantially OMW organic constituents, leading to a COD < 500 mg L⁻¹ and PP around 20 mg L⁻¹ in the final water. Considerable remediation was gained

also under simulated sunlight. As a remarkable advantage, a hybrid material made of ZY-supported anatase TiO₂ was for the first time applied for the *one-pot* treatment of OMW, under solar light. This material, combining solar light photocatalytic activity with sorption capacity, proved to be greatly advantageous in terms of efficiency, cost, ease of separation after use, and time-consumption.

Competing Interests

The authors declare that they have no competing interests.

Acknowledgments

The authors want to thank Dr. Alessandro Alloni for experimental support during his graduation thesis.

References

- [1] C. Pintucci, A. Giovannelli, M. L. Traversi, A. Ena, G. Padovani, and P. Carozzi, "Fresh olive mill waste deprived of polyphenols as feedstock for hydrogen photo-production by means of *Rhodospseudomonas palustris* 42OL," *Renewable Energy*, vol. 51, pp. 358–363, 2013.
- [2] I. Ntaikou, C. Kourmentza, E. C. Koutrouli et al., "Exploitation of olive oil mill wastewater for combined biohydrogen and biopolymers production," *Bioresource Technology*, vol. 100, no. 15, pp. 3724–3730, 2009.
- [3] S. Tosti, C. Accetta, M. Fabbicino, M. Sansovini, and L. Pontoni, "Reforming of olive mill wastewater through a Pd-membrane reactor," *International Journal of Hydrogen Energy*, vol. 38, no. 25, pp. 10252–10259, 2013.
- [4] G. Padovani, C. Pintucci, and P. Carozzi, "Dephenolization of stored olive-mill wastewater, using four different adsorbing matrices to attain a low-cost feedstock for hydrogen photo-production," *Bioresource Technology*, vol. 138, pp. 172–179, 2013.
- [5] P. Aytar, S. Gedikli, M. Sam, B. Farizoğlu, and A. Çabuk, "Sequential treatment of olive oil mill wastewater with adsorption and biological and photo-Fenton oxidation," *Environmental Science and Pollution Research*, vol. 20, no. 5, pp. 3060–3067, 2013.
- [6] E. De Marco, M. Savarese, A. Paduano, and R. Sacchi, "Characterization and fractionation of phenolic compounds extracted from olive oil mill wastewaters," *Food Chemistry*, vol. 104, no. 2, pp. 858–867, 2007.
- [7] L. Saez, J. Perez, and J. Martinez, "Low molecular weight phenolics attenuation during simulated treatment of wastewaters

- from olive oil mills in evaporation ponds,” *Water Research*, vol. 26, no. 9, pp. 1261–1266, 1992.
- [8] A. Speltini, M. Sturini, F. Maraschi et al., “Evaluation of UV-A and solar light photocatalytic hydrogen gas evolution from olive mill wastewater,” *International Journal of Hydrogen Energy*, vol. 40, no. 12, pp. 4303–4310, 2015.
- [9] M. O. J. Azzam, K. I. Al-Malah, and N. I. Abu-Lail, “Dynamic post-treatment response of olive mill effluent wastewater using activated carbon,” *Journal of Environmental Science and Health A*, vol. 39, no. 1, pp. 269–280, 2004.
- [10] C. C. Anastasiou, P. Christou, A. Michael, D. Nicolaidis, and T. P. Lambrou, “Approaches to olive mill wastewater treatment and disposal in Cyprus,” *Environmental Research Journal*, vol. 5, pp. 49–58, 2011.
- [11] P. S. Blika, K. Stamatelidou, M. Kornados, and G. Lyberatos, “Anaerobic digestion of olive mill wastewater,” *Global NEST Journal*, vol. 11, pp. 364–372, 2009.
- [12] R. C. Martins, A. M. Ferreira, L. M. Gando-Ferreira, and R. M. Quinta-Ferreira, “Ozonation and ultrafiltration for the treatment of olive mill wastewaters: effect of key operating conditions and integration schemes,” *Environmental Science and Pollution Research*, vol. 22, no. 20, pp. 15587–15597, 2015.
- [13] P. Canepa, F. Cauglia, P. Caviglia, and E. Chelossi, “Photo-Fenton oxidation of oil mill waste water: chemical degradation and biodegradability increase,” *Environmental Science and Pollution Research*, vol. 10, no. 4, pp. 217–220, 2003.
- [14] W. Gernjak, M. L. Maldonado, S. Malato et al., “Pilot-plant treatment of olive mill wastewater (OMW) by solar TiO₂ photocatalysis and solar photo-Fenton,” *Solar Energy*, vol. 77, no. 5, pp. 567–572, 2004.
- [15] L. Rizzo, G. Lofrano, M. Grassi, and V. Belgiorno, “Pre-treatment of olive mill wastewater by chitosan coagulation and advanced oxidation processes,” *Separation and Purification Technology*, vol. 63, no. 3, pp. 648–653, 2008.
- [16] C. I. Justino, K. Duarte, F. Loureiro et al., “Toxicity and organic content characterization of olive oil mill wastewater undergoing a sequential treatment with fungi and photo-Fenton oxidation,” *Journal of Hazardous Materials*, vol. 172, no. 2-3, pp. 1560–1572, 2009.
- [17] M. I. Badawy, F. E. Gohary, M. Y. Ghaly, and M. E. M. Ali, “Enhancement of olive mill wastewater biodegradation by homogeneous and heterogeneous photocatalytic oxidation,” *Journal of Hazardous Materials*, vol. 169, no. 1–3, pp. 673–679, 2009.
- [18] D. P. Zagklis, E. C. Arvaniti, V. P. Papadakis, and C. A. Paraskeva, “Sustainability analysis and benchmarking of olive mill wastewater treatment methods,” *Journal of Chemical Technology and Biotechnology*, vol. 88, no. 5, pp. 742–750, 2013.
- [19] M. Uğurlu and M. H. Karaoğlu, “TiO₂ supported on sepiolite: preparation, structural and thermal characterization and catalytic behaviour in photocatalytic treatment of phenol and lignin from olive mill wastewater,” *Chemical Engineering Journal*, vol. 166, no. 3, pp. 859–867, 2011.
- [20] E. Martini, M. Tomassetti, and L. Campanella, “Monitoring photocatalytic treatment of olive mill wastewater (OMW) in batch photoreactor using a tyrosinase biosensor and COD test,” in *Sensors and Microsystems*, vol. 268 of *Lecture Notes in Electrical Engineering*, pp. 169–173, Springer, 2014.
- [21] G. Rammohan and M. N. Nadagouda, “Green photocatalysis for degradation of organic contaminants: a review,” *Current Organic Chemistry*, vol. 17, no. 20, pp. 2338–2348, 2013.
- [22] M. Sturini, A. Speltini, F. Maraschi et al., “Photolytic and photocatalytic degradation of fluoroquinolones in untreated river water under natural sunlight,” *Applied Catalysis B: Environmental*, vol. 119–120, pp. 32–39, 2012.
- [23] M. Sturini, E. Rivagli, F. Maraschi, A. Speltini, A. Profumo, and A. Albini, “Photocatalytic reduction of vanadium(V) in TiO₂ suspension: chemometric optimization and application to wastewaters,” *Journal of Hazardous Materials*, vol. 254–255, no. 1, pp. 179–184, 2013.
- [24] A. A. Aly, Y. N. Y. Hasan, and A. S. Al-Farraj, “Olive mill wastewater treatment using a simple zeolite-based low-cost method,” *Journal of Environmental Management*, vol. 145, pp. 341–348, 2014.
- [25] J. Lin, Y. Zhan, Z. Zhu, and Y. Xing, “Adsorption of tannic acid from aqueous solution onto surfactant-modified zeolite,” *Journal of Hazardous Materials*, vol. 193, pp. 102–111, 2011.
- [26] V. Caratto, L. Setti, S. Campodonico, M. M. Carnasciali, R. Botter, and M. Ferretti, “Synthesis and characterization of nitrogen-doped TiO₂ nanoparticles prepared by sol-gel method,” *Journal of Sol-Gel Science and Technology*, vol. 63, no. 1, pp. 16–22, 2012.
- [27] F. Maraschi, M. Sturini, A. Speltini et al., “TiO₂-modified zeolites for fluoroquinolones removal from wastewaters and reuse after solar light regeneration,” *Journal of Environmental Chemical Engineering*, vol. 2, no. 4, pp. 2170–2176, 2014.
- [28] R. Asahi, T. Morikawa, T. Ohwaki, K. Aoki, and Y. Taga, “Visible-light photocatalysis in nitrogen-doped titanium oxides,” *Science*, vol. 293, no. 5528, pp. 269–271, 2001.
- [29] C. A. Santi, S. Cortes, L. P. D’Acqui, E. Sparvoli, and B. Pushparaj, “Reduction of organic pollutants in Olive Mill Wastewater by using different mineral substrates as adsorbents,” *Bioresource Technology*, vol. 99, no. 6, pp. 1945–1951, 2008.
- [30] E. Eroğlu, I. Eroğlu, U. Gündüz, and M. Yücel, “Effect of clay pretreatment on photofermentative hydrogen production from olive mill wastewater,” *Bioresource Technology*, vol. 99, no. 15, pp. 6799–6808, 2008.
- [31] V. Etacheri, C. Di Valentin, J. Schneider, D. Bahnemann, and S. C. Pillai, “Visible-light activation of TiO₂ photocatalysts: advances in theory and experiments,” *Journal of Photochemistry and Photobiology C: Photochemistry Reviews*, vol. 25, pp. 1–29, 2015.

